RSC Advances

ROYAL SOCIETY OF CHEMISTRY

www.rsc.org/advances

Gel-state 2D-NMR method for plant cell wall profiling and analysis: model study with the amorphous cellulose and xylan from ball-milled cotton linters

Hoon Kim*,[a] and John Ralph[a,b]
[a]Department of Biochemistry and the DOE Great Lakes Bioenergy Research Center, Wisconsin Energy Institute, 1552 University Ave, Madison, Wisconsin 53726, USA
[b]Department of Biological Systems Engineering, University of Wisconsin, Madison, Wisconsin 53706, USA

Proofs to:
Hoon Kim
Department of Biochemistry
University of Wisconsin, Madison
Wisconsin Energy Institute
1552 University Ave.
Madison, WI 53726
USA
Tel. (608) 263-0166
FAX: (608)-890-2270
Email: hoonkim@wisc.edu

John Ralph
Department of Biochemistry
University of Wisconsin, Madison
Wisconsin Energy Institute
1552 University Ave.
Madison, WI 53726
USA
Tel. (608) 890-2429
FAX: (608)-890-2270
Email: jralph@wisc.edu

Keywords
Gel-state 2D NMR, NUS (Non-Uniform Sampling), cellulose, xylan, cotton linters

RSC Advances

Version: Friday, Dec. 27, 2013 12:26 PM

Gel-state 2D-NMR method for plant cell wall profiling and analysis: model study with the amorphous cellulose and xylan from ball-milled cotton linters

Hoon Kim,* [a] *and John Ralph* [a,b]

[a]Department of Biochemistry and the DOE Great Lakes Bioenergy Research Center, Wisconsin Energy Institute, 1552 University Ave, Madison, Wisconsin 53726, USA

[b]Department of Biological Systems Engineering, University of Wisconsin, Madison, Wisconsin 53706, USA

Keywords:

Cellulose, xylan, cotton linters, cell wall dissolution, 2D NMR, NUS (Non-Uniform Sampling)

ABSTRACT

Recently developed "gel-state NMR method" that simply swells plant cell walls in DMSO-d_6/pyridine-d_5 (4:1) solvent system and uses high-resolution solution state 2D-NMR (HSQC) technique has been successfully applied to whole plant cell wall 2D-NMR profiling studies. However, there was limited information to assign many polysaccharide peaks unlike lignin structures. Here we collected NMR data from various cellulose and xylan models using the same

solvent system to assign the unknown peaks. Furthermore, DMSO-soluble cellulose and xylan fractions were prepared from ball-milled cotton linter cellulose, and the detailed chemical structures were analyzed. The major component of cotton is cellulose (95–99%), but it typically contains ~2% hemicelluloses. Xylan in particular was isolated and identified along with the amorphous cellulose in this study. The fully assigned spectra of cellulose and xylan provided invaluable database information for peak assignment and authentication that will be directly used to screen and identify the two main polysaccharide components from various whole cell wall NMR spectra in the same solvent system.

Introduction

Lignocellulosic biomass conversion has been a focus of study for sustainable energy research due to rising concerns over fossil fuel energy security and environmental issues.[1] Converting lignocellulosic biomass into various forms of alternative liquid fuels needs significant efforts to overcome many technical barriers. Although all of the major cell wall constituents (cellulose, hemicelluloses, and lignin) have been intensively studied, structurally assessing these complex polymers in the cell wall remains challenging.[2-4] Recent studies of transgenic and mutant plants have opened new windows to explore cell wall structure. As a consequence, an escalating number of research plant samples coming into facilities such as ours requires us to use more rapid, but still detailed, structural analysis methods. Recently, we developed "gel-state NMR method" that is a new high-resolution solution-state 2D NMR (HSQC) method for whole cell wall gel samples using DMSO-d_6 only or a DMSO-d_6/pyridine-d_5 (4:1) solvent system.[5-7] This method can deliver detailed structural information for lignins, including synthetic lignins (DHPs, dehydrogenation polymers),[8,9] and also the cell wall polysaccharides, hemicelluloses and

amorphous cellulose in an efficient way that can be applied to whole-cell wall samples without structural modification other than that caused by the ball-milling.[5,6,10-12] Many recent publications also established that this method can be independently applied to plant cell wall studies, isolated polysaccharide studies, and even water-insoluble metabolite studies.[13-16] A detailed structural study of amorphous cellulose and xylan, which are the most common cell wall components, using this potentially universal cell wall NMR solvent system is now needed to determine and validate assignments and support polysaccharide characterization research.

Cellulose is the major component of secondary walls in higher plants. It has a polymer chain of linear β-(1→4)-linked D-glucosyl (β-1,4-glucan) units, with a degree of polymerization (DP) of ~7,000-15,000.[17] It forms 15–30% of the primary cell wall and 35–50% of the secondary cell wall.[18] Cellulose also exists in the animal kingdom – in the tunicin from tunicates, for example.[19] Cellulose has different crystalline allomorphs. Cellulose I is natural cellulose with a crystalline structure.[20-22] Cellulose II refers to a thermodynamically stable structure with an antiparallel arrangement of the strands, characteristic of regenerated cellulose.[4,17] Amorphous cellulose (paracrystalline cellulose) is not as regular in structure compared to crystalline forms because the neighboring strands do not align as well, resulting in a less rigid structure, and making it more accessible to water.[4] It can be prepared by chemical or mechanical treatments; dimethylsulfoxide-paraformaldehyde,[23] cadmium ethylenediamine solution (Cadoxen),[24] cuprammonium hydroxide (Cuam, Cuoxam),[25] or ball-milling followed by dissolution in sodium hydroxide,[26] can all be used to generate amorphous cellulose.

NMR has long been an important tool for cellulose structural studies. Chemical shifts of highly crystalline cellulose II samples using solid-state CP/MAS ^{13}C-NMR were measured, and amorphous cellulose in DMSO was measured with solution-state ^{13}C-NMR.[27-29] However, un-

modified cellulose structures, and hemicelluloses such as xylan, have not been as well characterized with solution-state 2D NMR techniques.

Xylans are the most common of the hemicellulosic polymers. They have a backbone of xylopyranosyl residues that can be linked either via β-(1,3)- or β-(1,4)-linkages. However, all higher plants have a β-(1,4)-linked xylan as the backbone.[4,30] There are several types of xylans in the plants. Arabinoxylans (AXs), which exist in most grasses, including in cereal grains, have a xylan chain that is substituted with α-L-arabinofuranosyl units at the *O*-2 or *O*-3 positions.[30,31] Glucuronoarabinoxylans (GAXs) are structurally related to arabinoxylans, but they additionally have α-D-glucuronic acid (α-D-GlcA) substitutions on the xylan backbone. GAXs are the major cross-linking hemicellulosic polysaccharides in commelinoid monocots.[32] The α-L-arabinosyl residues are consistently linked to the xylosyl residue at the *O*-3 position. The α-D-GlcA residue is linked to the *O*-2 position of the xylan backbone. The arabinosyl unit can be further substituted with ferulate, which acylates the *O*-5 position of the arabinosyl unit. Such ferulates are involved in cross-linking of polysaccharide, forming diferulate bridges, and/or cross-linking of polysaccharides with lignin via oxidative radical coupling, and may act as nucleation sites for lignin polymerization in the cell walls of grasses.[33-36] Noncommelinoid monocots and all dicots also have GAX in which the α-L-arabinosyl residues are attached at either the *O*-2 or *O*-3 positions of xylan backbone.[4,37] 4-*O*-Methylglucuronoxylans (MGXs) are the most abundant type of hemicellulose in hardwood species, such as beech, birch and aspen.[38,39] These polysaccharides share the same β-(1,4)-linked D-xylan backbone as arabinoxylans (AXs) and glucuronoarabinoxylans (GAXs), but are substituted with 4-*O*-methyl-α-D-glucuronic acid (4-*O*-methyl-α-D-GlcA; 4-*O*-MeGlcA) residues instead of arabinose. Major xylan backbone structures have been characterized in NMR studies with a variety of solvent systems.[13,40-44]

For the study described here, we isolated the DMSO-soluble cellulose and xylan mixture from cotton linters. Cotton's major component is cellulose (95–99%), with an average DP (degree of polymerization) of close to 15,300.[17] Unlike cotton lint, cotton linters are short residual fibers that are attached to the cottonseed and they are produced by the delinting process before the seed is crushed to generate cottonseed oil.[45] Cotton linters typically contain ~2% hemicelluloses that may come from seed hulls.[45] On the other hand, cottonseed contains large amounts of xylan (40–45%), and its structure has been characterized as a glucuronoxylan, having both 4-*O*-MeGlcA and glucuronic acid (GlcA) substitutions.[46,47]

This paper reports the NMR data from various cellulose and xylan models and the complete peak assignments for the 2D NMR (HSQC) spectra of DMSO-soluble amorphous cellulose and xylan from cotton linter using the DMSO-d_6/pyridine-d_5 (4:1) solvent system, providing an assignment database for cell wall samples.

Results and Discussion

NMR Experiments for model compounds of cellulose and xylan

During the polysaccharide model study, one-dimensional (1D) ^{1}H and ^{13}C NMR experiments provided valuable information, but peak assignment is still not an easy task in the absence of multidimensional NMR techniques.[48] The NMR peak pattern becomes more complicated as the molecular weight of the polysaccharides increases. 2D NMR spectra provide invaluable information to provide assignments and to elucidate the structure of such polymers.[49] 2D HSQC spectra in particular can stand alone as a unique profiling method for polysaccharide structure.[50,51] The ^{1}H and ^{13}C NMR data for the polysaccharide models were collected from the 2D HSQC NMR spectra, and were directly used to elucidate the cotton linter polysaccharide

structures after completing the assignments (Table 1 & 2). HSQC experiments were for this model study were the same pulse experiments but parameters used were those used for small molecules rather than the fast-relaxing gel samples (see Experimental), and the HSQC data was supported by COSY experiments (not shown). We used the convenient and rather universal plant polymer solvent, DMSO-d_6/pyridine-d_5 (4:1),[6] for this study; the chemical shifts of polysaccharides are slightly different (about 1-2 ppm upfield for ^{13}C, and 0.1-0.2 ppm upfield for ^{1}H) from the chemical shifts that were obtained in D_2O, the solvent normally used for NMR studies of hemicellulosic components.

Characterization of cellulose model compounds

Polysaccharide model compounds, glucose, cellobiose, cellotriose, and cellotetraose, were subjected to NMR data collection in the DMSO-d_6/pyridine-d_5 (4:1) solvent system (Fig. S1 & S2). The 2D HSQC NMR peaks of α-D-glucose were easily identified via the complete proton assignments provided by COSY (^{1}H-^{1}H homonuclear coupling) experiments (not shown). After the α-D-glucose had been stored in the NMR tube for several days, some β-D-glucose was formed by anomerization, and the structure was identified from the α/β isomeric mixture. This provided a good starting point to achieve complete peak assignments for cellotriose and cellotetraose. Cellobiose already exhibited a complicated NMR spectrum (Table 1). As it has a reducing end and a non-reducing end without internal units, the C-NR_1 peak is new to cellobiose (over glucose), and is readily evident in the 2D-HSQC spectrum. Cellotriose (Fig. 2b & 3b) was the best model for recognizing all peaks from the cotton linter cellulose including the reducing end, non-reducing end, and the main internal backbone peaks. Cellotetraose provided the same peak patterns as seen from the cellotriose as the extra internal group (compared to the trimer) has

almost identical chemical shift data under these conditions (Fig. 1a, Fig. S1 & S2, Table 1). Quantitation of the anomeric internal unit peak (C-I_1) *vs* the non-reducing-end peak (C-NR_1) showed a corresponding ratio of 2:1 (C-I_1: C-NR_1) for cellotetraose and 1:1 (C-I_1: C-NR_1) for cellotriose. There is an interesting peak pattern for the non-reducing end (C-NR) and the reducing end (C-R) when they are compared to internal units (Fig. 1). The peaks C-R_4 and C-R_6 (both α and β anomers) from the reducing end overlapped (or closely located with) the internal unit (C-I_4 and C-I_6) peaks whereas other peaks, C-R_1, C-R_2, C-Rα_3, and C-R_5, were clearly separated from the corresponding internal peaks, and revealed themselves as the reducing-end peaks. C-Rβ_3 was almost overlapped with the internal peak (C-I_3), unlike C-Rα_3. The non-reducing-end peaks, C-NR_1, C-NR_2, and C-NR_5, overlapped with the corresponding internal peaks, C-I_1, C-I_2, and C-I_5. However, C-NR_3, C-NR_4, and C-NR_6 peaks were resolved from the corresponding internal groups and can therefore be recognized as unique 'marker peaks' for the non-reducing end. Those reducing-end and non-reducing-end peaks that overlapped with the internal peaks, were hard to distinguish from the internal backbone peaks of cellulose; however, the anomeric (C-NR_1) peak was readily distinguished. The peak assignment for models (Table 1) was verified by comparison with the assignments from previous cellulose-related polysaccharide studies.[49,52-54]

Characterization of xylan model compounds

Xylose, xylobiose, and xylotriose NMR data were also collected in the DMSO-d_6/pyridine-d_5 (4:1) solvent system (Fig. S1 & S2). β-D-Xylose also formed after the α-D-xylose was kept in the NMR tube for several days, and both the α and β anomeric structures were identified from the mixture. The same structural elucidation strategy as for the cellulose models was used for xylan

models; xylose NMR data was compared with the NMR data of xylobiose and xylotriose. Xylotriose (Fig. 2c & 3c) was the best model for the xylan-related peaks, as was cellotriose of cellulose-related peaks (Fig. 2b & 3b). However, the xylotriose non-reducing end (X-NR) and reducing end (X-R) behaved differently from the cellotriose. The anomeric internal unit peak (X-I_1) and the non-reducing-end peak (X-NR_1) shared the same chemical shifts at 101.98/4.35 ppm (C1/H1). The two reducing-end peaks (X-R_1 and X-R_2; both α and β isomers) were clearly distinguished from the corresponding internal peaks (X-I_1 and X-I_2). However, X-Rβ_3 and X-Rβ_5 coincided with their corresponding internal peaks whereas X-Rα_3 and X-Rα_5 were separated. X-R_4 (both α and β isomers) of the reducing end overlapped with the internal peak (X-I_4). Only two non-reducing-end peaks, X-NR_1 and X-NR_2, overlapped with the corresponding internal X-I_1 and X-I_2 peaks. Other peaks, X-NR_3, X-NR_4, and X-NR_5 were clearly separated from the internal peaks and easily recognized as the non-reducing-end peaks. The peak assignments (Table 2) were again verified from previous xylan studies.[43,55-57]

Birchwood xylan is pure 4-*O*-methylglucuronoxylan (MGX).[57,58] The xylan backbone NMR data was successfully obtained from this sample and helped to distinguish the xylan peaks in the polysaccharide mixtures (Fig. 2d & 3d).

2D-NMR Experiments for the mixture of cellulose and xylan from cotton linters

Ball-milled cellulose powder was prepared and dissolved in DMSO-d_6/pyridine-d_5 as described in the Experimental Section. The ground cellulose particle size was expected to be predominantly <10 μm as determined previously.[59] Many polysaccharides are soluble and can be extracted in alkali solution or hot water, but only some are soluble in DMSO.[60] We also found small amounts of polysaccharides to be soluble in DMSO-based solvents after a ball milling

process. We used the 'pure' cellulose from cotton linter for our extraction, and the DMSO-soluble fraction appears to be a 'successful mixture' of cellulose and xylan for this structural study. All of the polysaccharide model compounds, such as trimers and tetramers, readily dissolved in the DMSO-d_6/pyridine-d_5 solvent system.

Typical gel-state 2D HSQC NMR experimental parameters were used for the DMSO-extracted cellulose and xylan as described above.[5,6] Such NMR experimental parameters had been optimized for gel samples of ball-milled whole plant cell walls, and the advantage is the short acquisition time based on the rapid relaxation as a result of the high viscosity of the polymer. We optimized the single-scan acquisition times to as short as 100 ms in F2 (^{1}H), and used interscan relaxation delays (D1) of 500 ms, as explained in the NMR experimental section. The typical 5 h acquisition for the whole plant cell wall samples was sufficient for this cellulose and xylan sample to obtain all necessary correlations.

Adiabatic 2D HSQC NMR experiments run under typical conditions normally provide well-resolved resonances, but Non-Uniform Sampling (NUS) 2D HSQC NMR experiments were used here to provide significantly improved ^{13}C-dimension resolution without requiring additional NMR time. Non-Uniform Sampling has been long suggested as one method of improving both the resolution and the signal-to-noise ratio.[61,62] This newly-implemented Bruker standard NMR method allows high resolution along the indirect (^{13}C) dimension by sampling more data points in that dimension (equating to longer evolution times) without sampling the FID at each dwell-time-interval during the acquisition.[63] The NUS 2D HSQC NMR experiment provided clearly better resolution for the cotton linter polysaccharide sample.

Amorphous cellulose characterization

Despite the well-defined cellulose structure, only limited information on the NMR chemical shifts for non-derivatized cellulose in various NMR solvents can be found in the literature. Cellulose correlations in 2D HSQC NMR were assigned based on model studies here. Commercially available polysaccharide model compounds were tested in the DMSO-d_6/pyridine-d_5 solvent system as described later. The NMR chemical shift data for the amorphous cellulose are given in Table 3.

In the whole cell wall samples, most of the polysaccharide anomeric correlation peaks appear in the range of 90-106 ppm (^{13}C) and 3.7-6.0 ppm (^{1}H) in HSQC spectra. The structural changes and compositional distribution of polysaccharide backbone, branches between different species and samples can always be easily recognized.[6]

From the cotton linter sample, we were able to clearly identify the cellulose peaks, such as the internal peak, non-reducing-end peak, and both α and β reducing-end peaks (Fig. 2a).

The internal cellulose [C-I_1; (1→4)-β-D-Glc*p*] unit is the most important plant cell wall component; its anomeric (C1/H1) correlation peak appeared in spectra at 102.79/4.45 ppm. The same correlation appears, unsurprisingly, in the spectra from all plants we have surveyed.[5,6] The anomeric peak from the non-reducing-end terminal cellulose residues (C-NR_1) appeared at 103.18/4.38 ppm (C1/H1), and was extremely close to the internal cellulose peak (C-I_1). The cellulose DP (degree of polymer) was reasonably estimated as ~6 by integrating the non-reducing and internal anomeric peak; however, we are aware that the more mobile end-units may be over-quantitated by the NMR technique, so we assume that the actual DP is considerably higher.

The α- and β-anomer form reducing-end correlations of cellulose were clearly separated from those of the internal backbone units. A higher frequency of reducing ends will be present if there

are shorter polymers that are mostly produced from the ball-milling process. The C1/H1 correlation from the reducing-terminal-end of α-D-Glc*p* (C-Rα_1) was at 91.99/5.05 ppm (C1/H1); the analogous β-D-Glc*p* (C-Rβ_1) correlation was at 96.56/4.47 ppm (Fig. 2a, Table 3). The cellulose reducing-end peaks and xylan reducing-end peaks are quite close together, but they were readily differentiated and assigned.

The non-anomeric polysaccharide region (56-85/2.5-5.0 ppm) overlaps with the lignin side-chain region when whole cell wall samples are examined.[6]; there is, however, no lignin was discernible in the tested sample (Fig. 3a).

It is very difficult to resolve the polysaccharide peaks from whole cell wall samples in many cases because of the complexity and the many overlapping signals. However, most internal cellulose peaks in this region were clearly identified in the DMSO-d_6/pyridine-d_5 spectrum from the amorphous cellulose sample as major assigned peaks at 72.95/3.21 [C-I_2 (C2/H2)], 74.71/3.48 [C-I_3 (C3/H3)], 80.16/3.47 [C-I_4 (C4/H4)], 76.56/3.32 [C-I_5 (C5/H5)] ppm (Table 3); two internal C-I_6 (C6/H6) peaks were also distinctively located at 60.07/3.71 and 60.07/3.90 ppm. Most end-group correlations were well resolved, but some peaks were superimposed with other peaks. Non-reducing-end C-NR_6 (C6/H6) peaks were well separated from the internal C-I_6 (C6/H6) peaks and appeared at 60.85/3.53 and 60.85/3.82 ppm. C-NR_4 (C4/H4) was also clearly evident at 69.88/3.21 ppm, and C-NR_2 (C2/H2) was located close to the internal C-I_2 (C2/H2) at 73.15/3.15 ppm, but was reasonably resolved. However, C-NR_3 (C3/H3) and C-NR_5 (C5/H5) had coincident chemical shifts, and also overlapped with the internal C-I_5 (C5/H5) correlation at 76.56/3.32 ppm. The peak assignments for reducing ends were more complicated because these ends had α- and β-anomeric forms, unlike the non-reducing end. There were different chemical shift distribution patterns of the α and β anomeric peaks that will be discussed in the model study

section later. Despite the conformational complexity, however, all peaks were evidently assigned: 72.16/3.31 [C-Rα_2 (C2/H2)], 71.38/3.74 [C-Rα_3 (C3/H3)], and 69.82/3.85 [C-Rα_5 (C5/H5)] ppm. C-Rβ_2 (C2/H2) and C-Rβ_5 (C5/H5) were also well resolved at 74.40/3.13, 74.66/3.35 ppm. However, C-Rβ_3 (C3/H3) was coincident with C-I_3 at 74.91/3.44 ppm, C-Rα_4 (C4/H4) and C-Rβ_4 (C4/H4) were coincident at 80.57/3.46 ppm, and C-Rα_6 (C6/H6) and C-Rβ_6 (C6/H6) also were close together at 60.33/3.77 and 60.33/3.84 ppm, and were buried between the internal C-I_6 peaks.

Xylan characterization

Although most hemicelluloses have more complicated structures than cellulose, xylan structures have been well studied, and the internal backbone residues were clearly defined. However, detailed data for the xylan structures beyond the internal residue have again not been available, and incomplete NMR assignments have been commonly published in recent cell wall structural studies. By studying xylan models, we obtained some detailed information applicable to the isolated xylan from cotton linter. Furthermore, xylan from birch wood was an ideal standard to verify the internal (1→4)-β-D-Xyl*p* residue peaks (Fig. 2d & 3d). The NMR chemical shift data for the xylan are also given in Table 3, along with those of amorphous cellulose.

All xylan peaks were present in the same chemical shift range where the cellulose peaks appeared in the 2D HSQC NMR spectrum. Like cellulose, there were internal, non-reducing-end and both α and β reducing-end peaks (Fig. 2a).

The internal xylan correlation peak [X-I_1; (1→4)-β-D-Xyl*p*] from the backbone was at 101.63/4.37 ppm (C1/H1). Non-reducing-end xylan residues (X-NR_1), unfortunately, shared the same chemical shifts (Table 3). However, the xylan α- and β-anomer reducing-end correlations

appeared next to the cellulose reducing-end peaks and were clearly resolved. The α reducing-terminal-end of D-Xyl*p* (X-Rα_1) was at 92.26/5.00 ppm (C1/H1), and the correlation from the other reducing-terminal-end, β-D-Xyl*p* (C-Rβ_1), was present at 97.53/4.37 ppm (C1/H1). The xylan from the cotton linter was identified as a 4-*O*-methylglucuronoxylan (MGX) as is usually found in hardwoods.[30] The 2D NMR data of previously studied 4-*O*-methyl-α-D-glucuronic acid (4-*O*-MeGlcA; MGA) and the MGA branched β-D-Xyl*p* (X-MGA) were well matched with this current NMR data.[13,58] There were no traces of arabinofuranose (Ara*f*) peaks, which can usually be found in 4-*O*-methylglucuronoarabinoxylans (GAXs) or arabinoxylans (AXs).[64] in the range of 105-110 ppm (^{13}C) and 4.5-5.8ppm (^{1}H). This result corroborated the previous studies of cotton-seed xylan and simple glucuronoxylan, with 4-*O*-methylglucuronic acid (and glucuronic acid) structures found from acid and enzyme hydrolysis experiments.[46,47]

The xylan non-anomeric peaks also share the same chemical shift range (56-85/2.5-5.0 ppm) with cellulose non-anomerics and lignin side-chains. Despite the congestion of the correlations, most peaks were well resolved from the cellulose components and were readily assigned (Fig. 3a).

Two internal X-I_5 (C5/H5) peaks were located at 63.19/3.25 and 63.19/3.96 ppm. The internal residue of xylan backbone, X-I_2 (C2/H2), X-I_3 (C3/H3), and X-I_4 (C4/H4), appeared as major peaks at 72.55/3.19, 73.92/3.39, and 75.29/3.62 ppm, but X-I_2 shared its chemical shifts with other correlations. X-NR_2 (C2/H2), a non-reducing-end, appeared at ~72.55/3.19 ppm where the X-I_2 peak is, and C-I_2 (C2/H2), an internal cellulose peak, also appeared nearby. Other non-reducing-end peaks were clearly resolved from other correlations. X-NR_3 (C3/H3) and X-NR_4 (C4/H4) appeared at 76.26/3.26 and 69.43/3.41 ppm, and two X-NR_5 (C5/H5) peaks were located at 65.72/3.16 and 65.72/3.80 ppm. Peak assignment of reducing ends was also as

complicated as for cellulose because of the α- and β-anomers. X-Rα_2 (C2/H2) appeared at 72.16/3.31 ppm and is therefore in the same location as a cellulose reducing-end (C-Rα_2) peak. X-Rα_3 (C3/H3) was at 70.99/3.67 ppm, but the peak intensity was weak. Two X-Rα_5 (C5/H5) peaks appeared at 58.70/3.62 and 58.70/3.70 ppm; however, they also appeared near the noise level. X-Rβ_2 (C2/H2) appeared very close to C-Rβ_2 at 74.69/3.09 ppm, and the two X-Rβ_5 (C5/H5) also appeared right next to two X-I_5 peaks at 63.12/3.18 and 63.12/3.89 ppm. X-Rβ_3 (C3/H3) was fairly well resolved at 74.66/3.35 ppm, but it shared its chemical shifts with a cellulose reducing-end peak (C-Rβ_5). X-Rα_4 (C4/H4) and X-Rβ_4 (C4/H4) appeared with an internal xylan peak (X-I_4) at 75.29/3.62 ppm.

Absence of acetate groups in the cotton linter xylan

Although acetyl groups can easily be found in spectra from most plant cell walls, no acetates could be detected from the cotton linter xylan. The acetate methyl appears at ~20.7/1.97 ppm in plant cell wall samples. Most of the acetyl groups belong to hemicellulosic components and the naturally acetylated xylans can be easily detected in the non-anomeric regions of the spectra. Acetylated 4-*O*-methylglucuronoxylan is a major hemicellulosic component in hardwoods, and acetyl groups often acylate the C2 and C3 positions of xylosyl residues. NMR data for *O*-acetyl-(4-*O*-methyl-glucurono)-xylan in hardwoods have been reported.[39,56] A strong 2-*O*-Ac-β-D-Xyl*p* (C2/H2) correlation at 73.5/4.64 ppm and a 3-*O*-Ac-β-D-Xyl*p* (C3/H3) correlation at 75.0/4.94 ppm can be detected from the whole plant cell wall samples (Fig. 4B, b-d).[6] No such correlation peaks appear in the spectra from this sample. Possible degradation by solvents during the cellulose preparation may be the cause of the disappearance of such acetyl groups.

MGA (MeGlcA; 4-O-methyl-α-D-glucuronic acid) and X-MGA (MGA branched xylan)

Along with the acetyl group, 4-*O*-methyl-α-D-glucuronic acid (MeGlcA) and α-D-glucuronic acid (GlcA) are also near-ubiquitous components in many plants as components of their xylans.[55,65-69] A previous NMR study using the DMSO-d_6/pyridine-d_5 solvent system for Arabidopsis xylans isolated with KOH and 1% $NaBH_4$, also provided preliminary data for this structural study.[13] The distinctive anomeric peak (MGA_1) of MeGlcA was positioned at 97.34/5.24 ppm (C1/H1) (Fig. 2a). MGA_2 (C2/H2) appeared at 71.77/3.37 ppm and was close to the peak of C-Rα_2 and X-Rα_2. MGA_3 (C3/H3) was at 71.95/3.75 ppm right below the C-Rα_3 peak (Fig. 3a). MGA_4 (C4/H4), MGA_5 (C5/H5), and MGA_{OMe} peaks appeared clearly at 81.70/3.23, 69.69/4.68, and 59.09/4.43 ppm.[56,70] We estimated the ratio between the MeGlcA anomeric peak and the xylan backbone peak by NMR integration, revealing a frequency of one MeGlcA unit on every ~19 Xyl*p* residues. Commonly, one MeGlcA unit per 10-20 Xyl*p* residues are linked to the xylan chain by an α-(1→2)-linkage.[39,71,72]

When MeGlcA (or GlcA) is attached to an *O*-2 position of a xylan residue, the chemical shift of the xylan unit noticeably changes.[39,65,68,69,73,74] The X-MGA_1 correlation peak appeared next to the internal anomeric xylan (X-I_1) peak at 101.16/4.57 ppm (C1/H1). X-MGA_3 (C3/H3) and X-MGA_4 (C4/H4) also appeared close to the corresponding internal xylan peaks (X-I_3 and X-I_4) at 72.78/3.48 and 76.35/3.62 ppm. Two X-MGA_5 (C5/H5) peaks were at 62.60/3.34 and 62.60/4.12 ppm, right next to the internal xylan peaks (X-I_5). X-MGA_2 (C2/H2) was, logically, the peak most affected by the *O*-2 substitution. It moved far away from the original internal X-I_2 and appeared at 76.52/3.37 ppm.[55,75] These X-MGA structures were also examined in our previous research on isolated Arabidopsis xylans as described earlier.[13]

Whole cell walls comparison

The authenticated assignments obtained through the detailed 2D HSQC NMR results here will help to identify many of the common polysaccharide peaks that can be seen in diverse plant cell wall samples. Figure 4 shows a direct comparison between the cellulose & xylan standard NMR data derived here, and various plant cell walls that were prepared in previous gel-state 2D HSQC NMR studies of whole cell walls in DMSO-d_6/pyridine-d_5 (4:1).[6] As is now clear, the assignments in the cell wall systems can be more carefully and extensively made using this data.

Conclusions

Modern biomass and transgenic plant research demands the efficient analysis of plant cell wall composition and structure including polysaccharides. Polysaccharide model compounds and the isolated polysaccharides from the ball-milled cotton linter cellulose in DMSO-d_6/pyridine-d_5 (4:1) were used successfully to obtain detailed ^{13}C–^{1}H correlation spectra via solution-state 2D HSQC NMR experiments. The 2D NMR data revealed the structures of the mixture of amorphous cellulose and 4-*O*-methylglucuronoxylan from the cotton sample.

Using the DMSO-d_6/pyridine-d_5 (4:1) solvent system for polysaccharide research is a huge advantage for structural studies because the same NMR solvent has been successfully used for cell wall profiling research.[5,6,14] In other words, polysaccharide components can be easily profiled without complicated sample preparation or isolation processes, and without any of the chemical modifications that may accompany extraction methods. NMR profiling provides a simple but powerful method to obtain detailed information on complex cell wall composition and structure. Using DMSO-d_6/pyridine-d_5 (4:1) as the common solvent system would be beneficial for examining not only lignins but also polysaccharides in whole cell wall profiling studies.

Experimental

General

Reagents were from Aldrich (Milwaukee, WI, USA). Solvents used were AR grade and supplied by Fisher Scientific (Atlanta, GA, USA). Cellulose (microcrystalline, powder, 20 μm) from cotton linters, D-(+)-cellobiose, D-(+)-cellotetraose, D-(+)-xylose, D-(+)-glucose, and xylan from birch wood were purchased from Sigma-Aldrich (Milwaukee, WI, USA). D-(+)-Cellotriose, D-(+)-xylobiose, and D-(+)-xylotriose were purchased from Megazyme International Ireland Ltd. (Bray, Co. Wicklow, Ireland).

Cellulose and xylan model samples

D-(+)-Glucose, D-(+)-cellobiose, D-(+)-cellotriose, D-(+)-cellotetraose, D-(+)-xylose, D-(+)-xylobiose, and D-(+)-xylotriose were directly used to obtain 2D NMR spectra. Xylan from birch wood (2 g) was ground with a Retsch PM100 ball mill for 5 h 5 min (10 min grinding; 5 min break) as described above, and directly dissolved in DMSO-d_6/pyridine-d_5 (4:1) for NMR.

Preparation of DMSO-soluble cellulose and xylan from the cotton linters

The cellulose powder (2 g) was cryogenically pre-ground for 10 min (2 min grinding; 2 min break) at 30 Hz using a Retsch (Newtown, PA, USA) MM301 mixer mill with corrosion-resistant stainless steel screw-top grinding jars (50 ml) containing a single stainless steel ball bearing (30 mm). The pre-ground cellulose was then finely ground for 47 h 20 min (20 min grinding; 10 min break) using a Retsch PM100 planetary ball mill spinning at 600 rpm with zirconium dioxide (ZrO_2) vessels (50 ml) containing ZrO_2 ball bearings (10 mm × 10). The ball-

milled cellulose (1 g) was dissolved in DMSO (20 ml) for 3 days. Acetone (200 mL) was added into the DMSO solution, and the insoluble cotton cake was washed off with excess acetone. The DMSO solution was collected, and dried on a vacuum line over night after evaporating the acetone. A mixture of cellulose and xylan (5 mg) was obtained.

NMR Experiments

Polysaccharide samples were prepared directly in a 5 mm diameter NMR tube using the cell wall gel sample solution as originally described.[6] In general, pre-mixed DMSO-d_6/pyridine-d_5 (4:1) was used. Pyridine-d_5 with a purity of 99.5 atom% D was used for the polysaccharide samples whereas, for the whole plant cell wall samples (especially grass samples) that contained lignin components, we used pyridine-d_5 with enhanced purity ("100"; min. 99.94 atom% D) to avoid interference between the residual solvent peaks and certain correlations from aromatic moieties.

NMR experiments for polysaccharides from cotton were performed as previously described for the gel-state samples from ball-milled cell walls.[5,6] NMR spectra were acquired on a Bruker Biospin (Billerica, MA) Avance 500 MHz spectrometer fitted with a 5-mm TCI (triple resonance; ^{1}H, ^{13}C, ^{15}N) gradient cryoprobe with inverse geometry (proton coils closest to the sample). The central DMSO solvent peak was used as internal reference (δ_C 39.5, δ_H 2.49 ppm). The ^{13}C–^{1}H correlation experiment was an adiabatic HSQC experiment (Bruker standard pulse sequence 'hsqcetgpsisp.2'; phase-sensitive gradient-edited-2D HSQC using adiabatic pulses for inversion and refocusing).[76] HSQC experiments were carried out using the following parameters: acquired from 10 to 0 ppm in F2 (^{1}H) with 1000 data points (acquisition time 100 ms), 200 to 0 ppm in F1 (^{13}C) with 400 increments (F1 acquisition time 8 ms) of 72 scans with 500 ms

interscan delay; the d_{24} delay was set to 0.89 ms (1/8J, J = 145 Hz). The total acquisition time was 5 h. Processing used typical matched Gaussian apodization (GB = 0.001, LB = -0.1) in F2 and squared cosine-bell and one level of linear prediction (32 coefficients) in F1.

For the structural elucidation and assignment authentication of the model compounds, the number of scans can be adjusted as usual depending on the signal-to-noise required from a sample. The standard Bruker implementations of the traditional suite of 1D and 2D (gradient-selected, ^{1}H-detected, e.g., DEPT-135, COSY, HSQC, HSQC-TOCSY, HMBC) NMR experiments were used for model compounds. Adiabatic HSQC experiments (Bruker standard pulse sequence 'hsqcetgpsisp.2' or 'hsqcetgpsisp2.2') were also used for both model compounds and the cotton linter polysaccharide mixture sample and had the following parameters: spectra were acquired from 10 to 0 ppm in F2 (^{1}H) using 1998 data points for an acquisition time of ≤200 ms, 200 to 0 ppm in F1 (^{13}C) using 512 increments (F1 acquisition time 10.1 ms) of 8 scans with a 1 s interscan delay. The d_{24} delay was set to 0.89 ms (1/8J, J = 145 Hz). The total acquisition time was 1 h 24 min.

NUS (Non-Uniform Sampling) 2D NMR experiments were performed to obtain highly resolved data. The HSQC experiment was carried out using the following parameters: acquired from 10 to 0 ppm in F2 (^{1}H) with 1998 data points (acquisition time 200 ms), 200 to 0 ppm in F1 (^{13}C) with 1024 increments (F1 acquisition time 20.4 ms) of 64 scans with 1 s interscan delay; NUS, sampling 25% of the FID. NUS allowed a 2.6-fold TD1 (the number of points sampled in the second dimension) increase to improve resolution while reducing the total acquisition time from the normal HSQC experiment. The total acquisition time was 5 h 34 m for the higher S/N spectrum with two and a half times the F1 resolution.

Volume integration of contours in HSQC plots used the Bruker's TopSpin 3.1 (Mac version) software (on data upon which no linear prediction was applied).

Acknowledgements

This research was funded by the DOE Great Lakes Bioenergy Research Center (www.greatlakesbioenergy.org), which is supported by the U. S. Department of Energy, Office of Science, Office of Biological and Environmental Research, through Cooperative Agreement DE-FC02-07ER64494 between The Board of Regents of the University of Wisconsin System and the U.S. Department of Energy.

Notes and references

1 L. D. Schmidt and P. J. Dauenhauer, *Nature*, 2007, **447**, 914-915.
2 D. Fengel and G. Wegener, *Wood. Chemistry, Ultrastructure, Reactions*, Walter De Gruyter, Berlin-New York, 1989.
3 J. R. Obst, in *Forage Cell Wall Structure and Digestibility*, ed. H. G. Jung, D. R. Buxton, R. D. Hatfield and J. Ralph, ASA-CSSA-SSSA, Madison, WI, 1993, pp. 167-181.
4 W. Vermerris, in *Genetic Improvement of Bioenergy Crops*, ed. W. Vermerris, Springer New York, New York, 2008, pp. 89-142.
5 H. Kim, J. Ralph and T. Akiyama, *BioEnergy Research*, 2008, **1**, 56-66.
6 H. Kim and J. Ralph, *Organic & Biomolecular Chemistry*, 2010, **8**, 576-591.
7 S. D. Mansfield, H. Kim, F. C. Lu and J. Ralph, *Nature Protocols*, 2012, **7**, 1579-1589.
8 J. H. Grabber, D. R. Mertens, H. Kim, C. Funk, F. Lu and J. Ralph, *Journal of the Science of Food and Agriculture*, 2009, **89**, 122-129.
9 J. H. Grabber, P. F. Schatz, H. Kim, F. Lu and J. Ralph, *BMC Plant Biology*, 2010, **10**, 1-13.
10 J. Rencoret, G. Marques, A. Gutierrez, L. Nieto, J. I. Santos, J. Jimenez-Barbero, A. T. Martinez and J. C. del Rio, *Holzforschung*, 2009, **63**, 691-698.
11 J. Rencoret, A. Gutiérrez, L. Nieto, J. Jiménez-Barbero, C. B. Faulds, H. Kim, J. Ralph, Á. T. Martínez and J. C. del Río, *Plant Physiology*, 2011, **155**, 667-682.
12 A. T. Martinez, J. Rencoret, L. Nieto, J. Jimenez-Barbero, A. Gutierrez and J. C. del Rio, *Environmental Microbiology*, 2011, **13**, 96-107.
13 J. K. Jensen, H. Kim, J.-C. Cocuron, R. Orler, J. Ralph and C. G. Wilkerson, *The Plant Journal*, 2011, 387-400.
14 M. Brennan, J. P. McLean, C. M. Altaner, J. Ralph and P. J. Harris, *Cellulose*, 2012, **19**, 1385-1404.
15 Y. Date, K. Sakata and J. Kikuchi, *Polymer Journal*, 2012, **44**, 888-894.

16 B. R. Urbanowicz, M. J. Pena, S. Ratnaparkhe, U. Avci, J. Backe, H. F. Steet, M. Foston, H. J. Li, M. A. O'Neill, A. J. Ragauskas, A. G. Darvill, C. Wyman, H. J. Gilbert and W. S. York, *Proceedings of the National Academy of Sciences of the United States of America*, 2012, **109**, 14253-14258.
17 D. Fengel and G. Wegener, in *Wood. Chemistry, Ultrastructure, Reactions*, Walter De Gruyter, Berlin-New York, 1989, pp. 66-105.
18 J. Vogel, *Current Opinion in Plant Biology*, 2008, **11**, 301-307.
19 A. B. Wardrop, *Protoplasma*, 1970, **70**, 73-86.
20 R. H. Atalla and D. L. VanderHart, *Solid State Nuclear Magnetic Resonance* 1999, **15**, 1-19.
21 J. J. Sugiyama, R. Vuong and H. Chanzy, *Macromolecules*, 1991, **24**, 4168-4175.
22 R. J. Viëtor, R. H. Newman, M.-A. Ha, D. C. Apperley and M. C. Jarvis, *The Plant Journal*, 2002, **30**, 721-731.
23 L. R. Schroeder, V. M. Gentile and R. H. Atalla, *J. Wood Chem. Technol.*, 1986, **6**, 1-14.
24 A. Jeziorny and S. Kepka, *J. Polym. Sci., Polym. Lett.*, 1972, **10**, 257-260.
25 R. Jeffries, *J. Appl. Polym. Sci.*, 1968, **12**, 425-445.
26 P. H. Hermans and A. Weidinger, *J. Am. Chem. Soc.*, 1946, **68**, 2547-2552.
27 A. Isogai, T. Kato, T. Uryu and R. H. Atalla, *Carbohydrate Polymers*, 1993, **21**, 277-281.
28 J. S. Moulthrop, R. P. Swatloski, G. Moyna and R. D. Rogers, *Chemical Communications*, 2005, 1557-1559.
29 B. Böck, S. Böck and D. Fengel, *Holzforschung*, 1991, **45**, 321-324.
30 A. Ebringerová and T. Heinze, *Macromol. Rapid Commun.*, 2000, **21**, 542-556.
31 C. D. Nandini and P. V. Salimath, *J. Agric. Food Chem.*, 2002, **50**, 6485−6489.
32 N. C. Carpita and M. C. McCann, *Plant and Soil*, 2002, **247**, 71-80.
33 K. Iiyama, T. B. T. Lam and B. Stone, *Plant Physiol*, 1994, **104**, 315-320.
34 J. H. Grabber, J. Ralph and R. D. Hatfield, *J. Agric. Food Chem.*, 2002, **50**, 6008-6016.
35 R. D. Hatfield, J. Ralph and J. H. Grabber, *J. Sci. Food Agric.*, 1999, **79**, 403-407.
36 J. Ralph, *Phytochemistry Reviews*, 2010, **9**, 65-83.
37 N. C. Carpita and M. C. McCann, in *Biochemistry and Molecular Biology of Plants*, ed. B. B. Buchanan, W. Gruissem and R. L. Jones, J. Wiley and Sons, Somerset, NJ, 2000, pp. 52–108.
38 P. Westbye, T. K□hnke and P. Gatenholm, *Holzforschung*, 2008, **62**, 31-37.
39 A. Teleman, M. Tenkanen, A. Jacobs and O. Dahlman, *Carbohydrate Research*, 2002, **337**, 373-377.
40 R. A. Hoffmann, T. Geijtenbeek, J. P. Kamerling and J. F. G. Vliegenthart, *Carbohydr. Res.*, 1992, **223**, 19-44.
41 T. Nishimura, M. Ishihara, T. Ishii and A. Kato, *Carbohydrate Research*, 1998, **308**, 117-122.
42 M. J. Peña, R. Zhong, G.-K. Zhou, E. A. Richardson, M. A. O'Neill, A. G. Darvill, W. S. York and Z.-H. Ye, *The Plant Cell*, 2007, **19**.
43 T. Ishii, T. Konishi, H. Ono, M. Ohnishi-Kameyama, H. Togashi and K. Shimizu, *Carbohydrate Polymers* 2008, **74**, 579–589.
44 H. Komiyama, A. Enomoto, Y. Sueyoshi, T. Nishio, A. Kato, T. Ishii and K. Shimizu, *Carbohydrate Polymers*, 2009, **75**.
45 A. Sczostak, *Macromolecular Symposia*, 2009, **280**, 45-53.
46 N. Matsuo, S. Yoshida, I. Kusakabe and K. Murakami, *Agric. Biol. Chem.*, 1991, **55**, 2905-2907.

47 H. J. Sun, S. Yoshida, N.-H. Park and I. Kusakabe, *Carbohydrate Research*, 2002, **337**, 657–661.
48 B. Mulloy, *Molecular Biotechnology*, 1996, **6**, 241-265.
49 L. A. Flugge, J. T. Blank and P. A. Petillo, *J. Am. Chem. Soc.*, 1999, **121**, 7228-7238.
50 M. Hedenström, S. Wiklund-Lindstrom, T. Öman, F. Lu, L. Gerbner, P. F. Schatz, B. Sundberg and J. Ralph, *Molecular Plant*, 2009, **2**, 933-942.
51 R. A. Chylla, R. Van Acker, H. Kim, A. Azapira, P. Mukerjee, J. L. Markley, V. Storme, W. Boerjan and J. Ralph, *Biotechnology for Biofuels*, 2013, **6**.
52 P. E. Pfeffer, K. M. Valentine and F. W. Parrish, *J. Am. Chem. Soc.*, 1979, **28**, 1265-1274.
53 L. D. Hall, G. A. Morris and S. Sukumar, *J. Am. Chem. Soc.*, 1980, **93**, 1745–1747.
54 M. Ikura and K. Hikichi, *Carbohydrate research*, 1987, **163**, 1-8.
55 J. P. Utille, P. Kovac, F. Sauriol and A. S. Perlin, *Carbohydrate Research*, 1986, **154**, 251-258.
56 A. Teleman, J. Lundqvist, F. Tjerneld, H. Stålbrand and O. Dahlman, *Carbohydrate Research*, 2000, **329**, 807-815.
57 K. Petzold, W. Gunther, M. Kotteritzsch and T. Heinze, *Carbohydrate Polymers*, 2008, **74**, 327-332.
58 F. Cavagna, H. Deger and J. Puls, *Carbohydrate Research*, 1984, **129**, 1-8.
59 F. H. Forziati, W. K. Stone, J. W. Rowen and W. D. Appel, *Journal of Research of the National Institute of Standards and Technology*, 1950, **45**, 109-113.
60 E. Sjöström, in *Wood chemistry - Fundamentals and applications*, Academic Press, Inc., San Diego, Second edition edn., 1993, pp. 51-70.
61 Y. Manassen, G. Navon and C. T. W. Moonen, *Journal of Magnetic Resonance*, 1987, **72**, 551-555.
62 Y. Manassen and G. Navon, *Journal of Magnetic Resonance*, 1988, **79**, 291-298.
63 A. D. Schuyler, M. W. Maciejewski, H. Arthanari and J. C. Hoch, *Journal of Biomolecular NMR*, 2011, **50**, 247-262.
64 A. Ebringerová, Z. Hromádková and T. Heinze, *Adv. Polym. Sci.*, 2005, **186**, 1-67.
65 P. Debeire, B. Priem, G. Strecker and M. Vignon, *European Journal of Biochemistry*, 1990, **187**, 573-580.
66 B. Lindberg, M. Mosihuzzaman, N. Nahar, R. M. Abeysekera, R. G. Brown and J. H. M. Willison, *Carbohydrate Research*, 1990, **207**, 307-310.
67 N. R. Swamy and P. V. Salimath, *Carbohydrate Research*, 1990, **197**, 327-337.
68 A. Bazus, L. Rigal, A. Gaset, T. Fontaine, J. M. Wieruszeski and B. Fournet, *Carbohydrate Research*, 1993, **243**, 323-332.
69 M. R. Vignon and C. Gey, *Carbohydrate Research*, 1998, **307**, 107-111.
70 Y. Habibi and M. R. Vignon, *Carbohydrate Research*, 2005, 1431-1436.
71 B. W. Simson and T. E. Timell, *Cellulose Chemistry and Technology*, 1978, **12**.
72 T. E. Timell, *Wood Science and Technology*, 1967, **1**.
73 Y. Habibi, M. Mahrouz and M. R. Vignon, *Carbohydrate Research*, 2002, **337**, 1593-1598.
74 T. Ishii, T. Konishi, T. Yamasaki, A. Enomoto, M. Yoshida, I. Maeda and K. Shimizu, *Carbohydrate Polymers*, 2010, **81**, 964-968.
75 K. Mizutani, A. Hayashi, R. Kasai, O. Tanaka, N. Yoshida and T. Nakajima, *Carbohydrate Research*, 1984, **126**, 177-189.
76 E. Kupče and R. Freeman, *J. Magn. Reson.*, 2007, **187**, 258-265.

Figure captions

Fig. 1. Structures of cellulose and xylan model compounds. The chemical shift behavior of the terminal and internal units was distinguished via the positions delineated by the dotted lines, i.e., a part of the reducing end and the non-reducing end units has completely different chemical shifts from the corresponding positions in the internal units. Each internal unit shares the same chemical shift peaks, and that results in increased correlation intensities in the backbone peaks with increased polymer size.

Fig. 2. Anomeric region of 2D $^{13}C–^{1}H$ correlation (HSQC) spectra of cellulose and xylan from cotton linter polysaccharides and other polysaccharide models in DMSO-d_6/pyridine-d_5 (4:1). a) cotton linter, b) cellotriose, c) xylotriose, d) Birchwood xylan. The assignments are based on NMR data from model compounds (Fig. 1) in the same solvent, and from other references.

Fig. 3. Non-anomeric region (aliphatic regions for whole plant cell wall samples) of the 2D $^{13}C–^{1}H$ correlation (HSQC) spectra from the cell wall gels and soluble lignins from cotton linter polysaccharides and other polysaccharide models in DMSO-d_6/pyridine-d_5 (4:1). a) cotton linter, b) cellotriose, c) xylotriose, d) Birchwood xylan. C-I, cellulose internal unit; C-NR, cellulose non-reducing end unit; C-Rα, cellulose α reducing end unit; C-Rβ, cellulose β reducing end unit; X-I, xylose internal unit; X-NR, xylan non-reducing end unit; X-Rα, xylan α reducing end unit; X-Rβ, xylan β reducing end unit; MGA, 4-*O*-methyl-α-D-glucuronic acid (4-*O*-MeGlcA); X-MGA, MGA branched β-D-Xylp; R, reducing end; NR, non-reducing end.

Fig. 4. 2D HSQC NMR spectra of whole plant cell walls that contain lignins and polysaccharides were compared with the cotton linter cellulose and xylan (a). A; anomeric region. 2D NMR spectra

revealing polysaccharide anomerics. Partial short-range $^{13}C–^{1}H$ (HSQC) spectra (polysaccharide anomeric regions) of cell wall gel samples (b–d). The common polysaccharide nomenclature is used. Some correlations (labeled as ?, or unlabeled) remain uncertain or unidentified. B; non-anomeric region. Lignin correlations are labeled L, with color-coded structures as given. General polysaccharide assignments are given, along with the diagnostic correlations for the acetylated xylan (in poplar and corn).

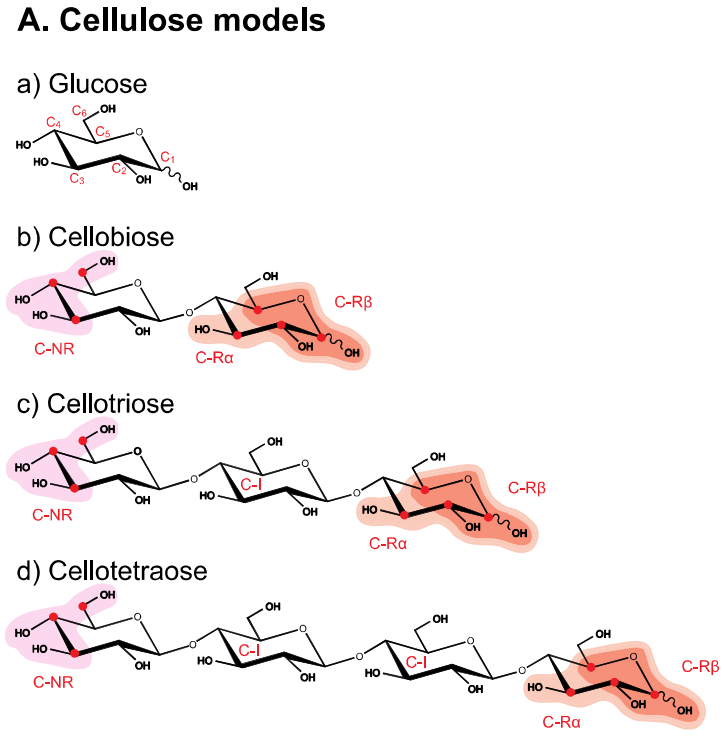

Figure 1

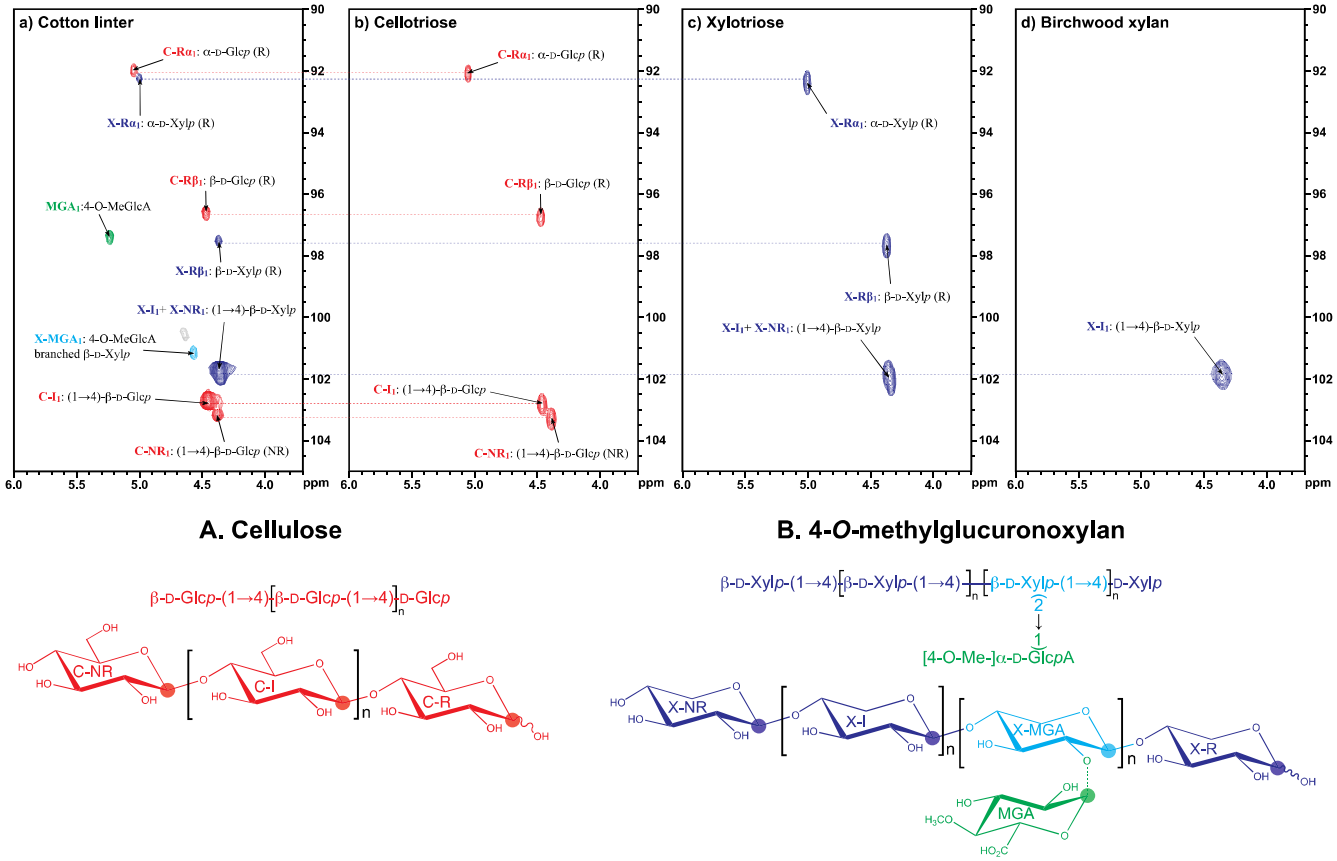

Figure 2

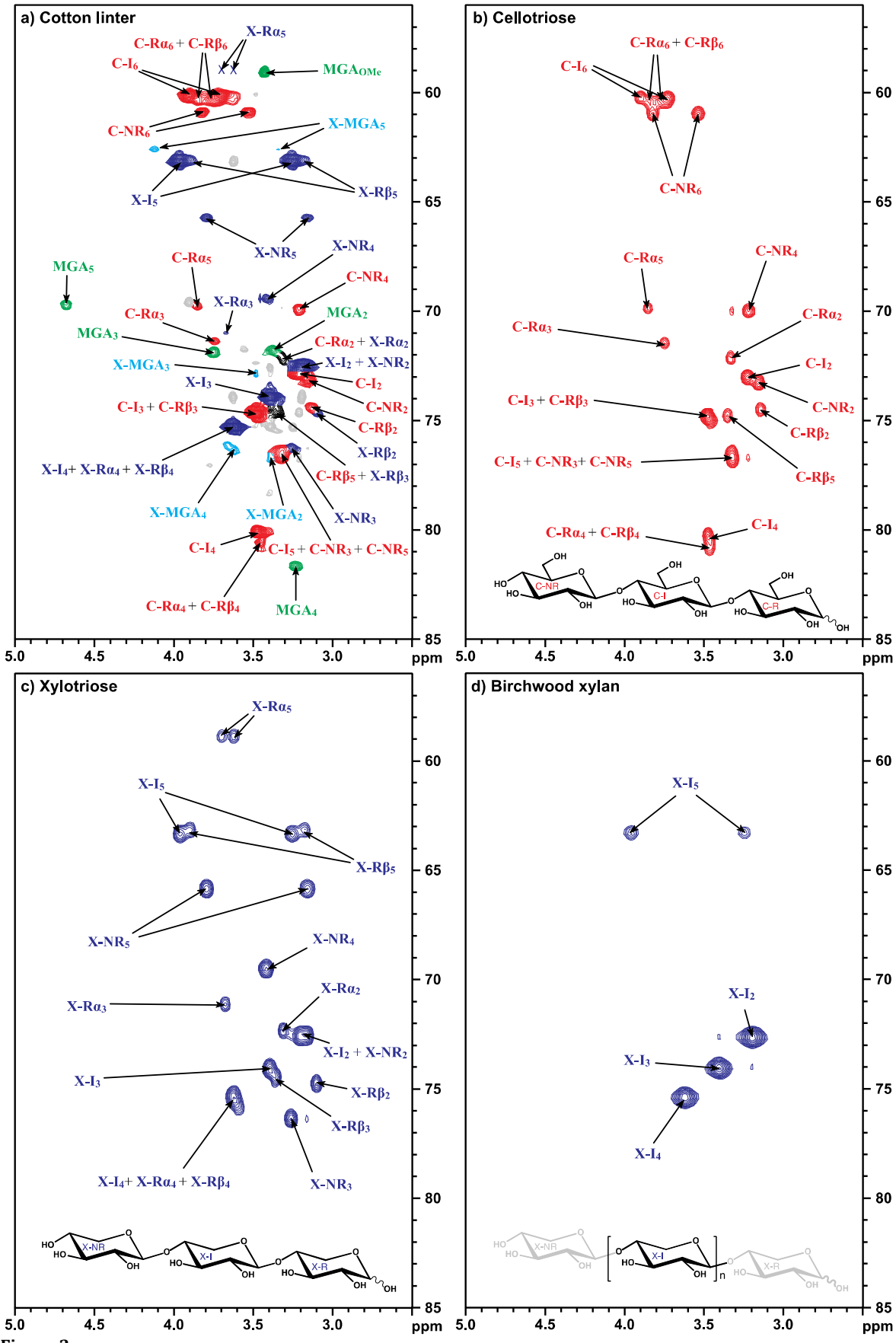

Figure 3

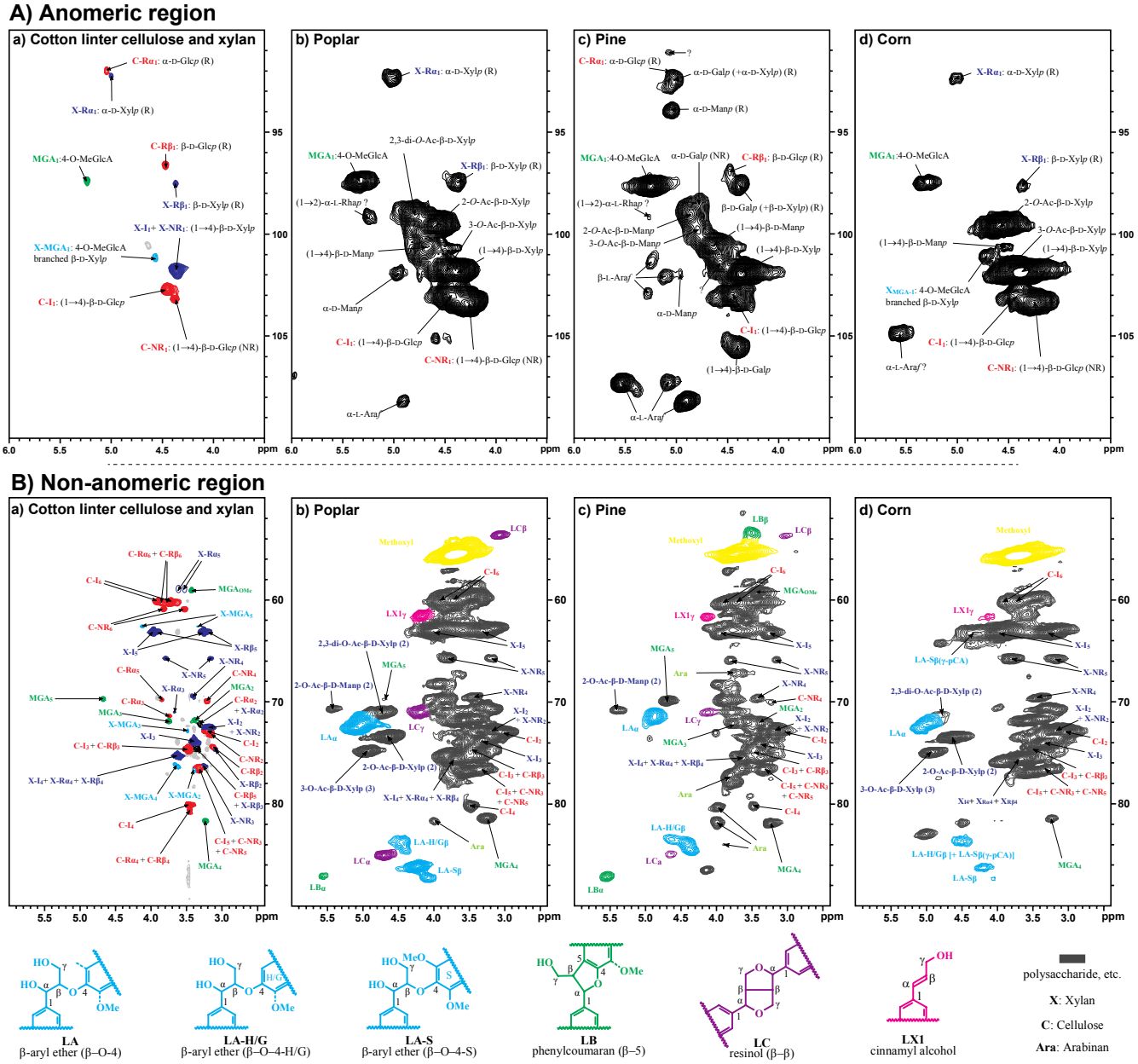

Figure 4

Table 1. NMR data for cellulose models in DMSO-d_6/pyridine-d_5 (4:1)

Cellulose model compound residue		^{1}H & ^{13}C Chemical shifts (ppm)								
		1	**2**	**3**	**4**	**5a**	**5b**	**6a**	**6b**	**OMe**
Glucose (α)	^{1}H	5.13	3.35	3.71	3.31	3.80	–	3.65	3.78	–
	^{13}C	92.61	72.70	73.49	70.80	72.22	–	61.50	61.50	–
Glucose (β)	^{1}H	4.50	3.16	3.37	3.28	3.28	–	3.61	3.84	–
	^{13}C	97.18	75.14	77.01	70.53	76.96	–	61.45	61.45	–
Cellobiose (Rα)	^{1}H	5.05	3.34	3.75	3.45	3.86	–	3.74	3.85	–
	^{13}C	92.08	72.14	71.46	80.66	69.81	–	60.52	60.52	–
Cellobiose (Rβ)	^{1}H	4.48	3.14	3.45	3.45	3.36	–	3.74	3.85	–
	^{13}C	96.69	74.51	75.00	80.66	74.76	–	60.52	60.52	–
Cellobiose (NR)	^{1}H	4.40	3.17	3.33	3.23	3.33	–	3.54	3.83	–
	^{13}C	103.24	73.23	76.63	69.94	76.63	–	60.91	60.91	–
Cellotriose (Rα)	^{1}H	5.05	3.33	3.75	3.46	3.85	–	3.80	3.84	–
	^{13}C	92.10	72.13	71.51	80.77	69.88	–	60.37	60.37	–
Cellotriose (Rβ)	^{1}H	4.47	3.14	3.45	3.46	3.35	–	3.80	3.84	–
	^{13}C	96.74	74.51	75.10	80.77	74.79	–	60.37	60.37	–
Cellotriose (internal)	^{1}H	4.46	3.23	3.48	3.48	3.32	–	3.74	3.90	–
	^{13}C	102.86	73.04	74.81	80.28	76.72	–	60.29	60.29	–
Cellotriose (NR)	^{1}H	4.39	3.16	3.32	3.22	3.32	–	3.54	3.82	–
	^{13}C	103.32	73.25	76.72	69.95	76.72	–	60.94	60.94	–
Cellotetraose (Rα)	^{1}H	5.07	3.36	3.77	3.49	3.88	–	3.78	3.86	–
	^{13}C	92.10	72.13	71.46	80.82	69.88	–	60.46	60.46	–
Cellotetraose (Rβ)	^{1}H	4.50	3.16	3.48	3.49	3.37	–	3.78	3.86	–
	^{13}C	96.74	74.54	75.15	80.82	74.77	–	60.46	60.46	–
Cellotetraose (internal 1 & 2)	^{1}H	4.48	3.24	3.50	3.50	3.34	–	3.74	3.92	–
	^{13}C	102.89	72.99	74.78	80.23	76.68	–	60.22	60.22	–
Cellotetraose (NR)	^{1}H	4.40	3.18	3.34	3.24	3.34	–	3.55	3.85	–
	^{13}C	103.31	73.22	76.68	69.99	76.68	–	60.92	60.92	–

R; reducing end, NR; non-reducing end

Table 2. NMR data for xylan models in DMSO-d_6/pyridine-d_5 (4:1)

Xylan model compound residue		^{1}H & ^{13}C Chemical shifts (ppm)								
		1	**2**	**3**	**4**	**5a**	**5b**	**6a**	**6b**	**OMe**
Xylose (α)	^{1}H	5.00	3.28	3.57	3.39	3.47	3.62	–	–	–
	^{13}C	92.68	72.46	73.43	70.28	61.62	61.62	–	–	–
Xylose (β)	^{1}H	4.36	3.06	3.23	3.40	3.10	3.72	–	–	–
	^{13}C	97.87	74.86	76.92	69.92	65.82	65.82	–	–	–
Xylobiose (Rα)	^{1}H	5.01	3.32	3.68	3.59	3.62	3.71	–	–	–
	^{13}C	92.36	72.33	71.09	75.81	58.87	58.87	–	–	–
Xylobiose (Rβ)	^{1}H	4.38	3.10	3.37	3.61	3.18	3.90	–	–	–
	^{13}C	97.64	74.74	74.49	75.54	63.20	63.20	–	–	–
Xylobiose (NR)	^{1}H	4.33	3.17	3.26	3.42	3.16	3.80	–	–	–
	^{13}C	102.08	72.49	76.35	69.47	65.78	65.78	–	–	–
Xylotriose (Rα)	^{1}H	5.00	3.31	3.68	3.60	3.62	3.70	–	–	–
	^{13}C	92.39	72.32	71.14	75.75	58.85	58.85	–	–	–
Xylotriose (Rβ)	^{1}H	4.37	3.10	3.36	3.62	3.18	3.90	–	–	–
	^{13}C	97.69	74.76	74.44	75.41	63.16	63.16	–	–	–
Xylotriose (internal)	^{1}H	4.35	3.20	3.40	3.62	3.25	3.96	–	–	–
	^{13}C	101.98	72.59	74.07	75.41	63.31	63.31	–	–	–
Xylotriose (NR)	^{1}H	4.35	3.16	3.26	3.42	3.16	3.80	–	–	–
	^{13}C	101.98	72.59	76.38	69.53	65.86	65.86	–	–	–
Xylan (Birchwood)	^{1}H	4.36	3.19	3.40	3.62	3.24	3.96	–	–	–
	^{13}C	101.83	72.67	74.09	75.42	63.30	63.30	–	–	–
MGA (NR)	^{1}H	5.23	3.36	3.74	3.23	4.65	–	–	–	3.43
	^{13}C	97.61	71.99	72.08	81.90	70.02	–	–	–	59.25
X_{MGA} (internal)	^{1}H	4.57	3.35	3.48	3.61	3.34	4.11	–	–	–
	^{13}C	101.28	76.70	72.53	76.51	62.76	62.76	–	–	–

R; reducing end, NR; non-reducing end, MGA; 4-*O*-Me-α-D-Glc*p*A (MeGlcA), X_{MGA}; 4-*O*-Me-α-D-Glc*p*A linked *O*-2 to (1→4)-β-D-Xyl*p* (α-(1→2)-linkage), MGA (NR) and X_{MGA} (internal) assignment was based on previous xylan 2D NMR study (2011, Jensen et al., The plant journal, 66, 387-400).

Table 3. NMR data for polysaccharide components in the cotton linter in DMSO-d_6/pyridine-d_5 (4:1)

Glycosyl residue		^{1}H & ^{13}C Chemical shifts (ppm)								
		1	**2**	**3**	**4**	**5a**	**5b**	**6a**	**6b**	**OMe**
Cellulose (internal)	^{1}H	4.45	3.21	3.48	3.47	3.32	–	3.71	3.90	–
	^{13}C	102.79	72.95	74.71	80.16	76.56	–	60.07	60.07	–
Cellulose (NR)	^{1}H	4.38	3.15	3.32	3.21	3.32	–	3.53	3.82	–
	^{13}C	103.18	73.15	76.56	69.88	76.56	–	60.85	60.85	–
Cellulose (Rα)	^{1}H	5.05	3.31	3.74	3.46	3.85	–	3.77	3.84	–
	^{13}C	91.99	72.16	71.38	80.57	69.82	–	60.33	60.33	–
Cellulose (Rβ)	^{1}H	4.47	3.13	3.44	3.46	3.35	–	3.77	3.84	–
	^{13}C	96.56	74.40	74.91	80.57	74.66	–	60.33	60.33	–
Xylan (internal)	^{1}H	4.37	3.19	3.39	3.62	3.25	3.96	–	–	–
	^{13}C	101.63	72.55	73.92	75.29	63.19	63.19	–	–	–
Xylan (NR)	^{1}H	4.37	3.19	3.26	3.41	3.16	3.80	–	–	–
	^{13}C	101.63	72.55	76.26	69.43	65.72	65.72	–	–	–
Xylan (Rα)	^{1}H	5.00	3.31	3.67	3.62	3.62	3.70	–	–	–
	^{13}C	92.26	72.16	70.99	75.29	58.70	58.70	–	–	–
Xylan (Rβ)	^{1}H	4.37	3.09	3.35	3.62	3.18	3.89	–	–	–
	^{13}C	97.53	74.69	74.66	75.29	63.12	63.12	–	–	–
MGA (NR)	^{1}H	5.24	3.37	3.75	3.23	4.68	–	–	–	3.43
	^{13}C	97.34	71.77	71.95	81.70	69.69	–	–	–	59.09
X_{MGA} (internal)	^{1}H	4.57	3.37	3.40	3.62	3.34	4.12	–	–	–
	^{13}C	101.16	76.52	72.58	76.35	62.60	62.60	–	–	–

Cellulose; (1→4)-β-D-Glc*p*, Xylan; (1→4)-β-D-xyl*p*, NR; non-reducing end, R; reducing end, MGA; 4-*O*-Me-α-D-Glc*p*A (MeGlcA), X_{MGA}; 4-*O*-Me-α-D-Glc*p*A linked *O*-2 to (1→4)-β-D-Xyl*p* (α-(1→2)-linkage)

TOC

Amorphous cellulose and xylan structures were analyzed using high-resolution 2D-NMR, and the NMR data were obtained in DMSO-d_6/pyridine-d_5 (4:1) solvent system.